Modeling of Joule Heating in Electrophoretic Separation Microchips

Yi Wang, Qiao Lin, James F. Hoburg and Tamal Mukherjee
Carnegie Mellon University, Pittsburgh, PA, USA. yiw@andrew.cmu.edu

ABSTRACT

This paper presents a model for Joule heating induced analyte dispersion in electrophoretic separation channels with a rectangular cross section. The model is in closed form and captures the effect of cross-sectional geometry. Three-dimensional numerical simulations are performed to satisfactorily verify the model, which can be used to accurately predict the performance of high speed electrophoretic separations.

Keywords: band broadening, band spreading, dispersion, electrophoresis, Joule heating, microchip.

1   INTRODUCTION

Joule heating (JH) at high electric fields is a major problem in microchip electrophoretic separations. For example, in ultra fast electrophoresis [1] and constricted bend designs used for minimizing turn-induced dispersion [2], variations of analyte velocity within the microchannel cross section may induce convective dispersion of the analyte, causing significant spreading of the analyte band. Previously, convective dispersion of analytes has been investigated mostly for capillaries with a circular cross section. Taylor [3,4] and Aris [5] derived a dispersion coefficient analogous to the diffusivity in pure diffusion. Their approach was later adopted to develop a JH induced analyte dispersion model in circular capillaries [6]. While this model has been used to study high speed electrophoresis microchip [1], it is in general inappropriate for micromachined channels typically having a noncircular cross section. There have been efforts to consider dispersion induced band spreading in noncircular geometries (e.g., [2,7]), but Joule heating effects have not been adequately investigated. Recognizing this practical need, we present a closed-form model for JH dispersion in rectangular micro channels. The model captures the effect of cross-sectional geometry on JH dispersion and can

accurately predict the performance of high speed electrophoretic separations.
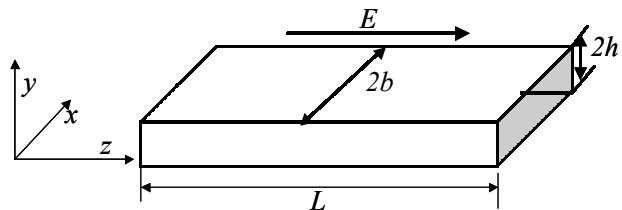
2   PROBLEM FORMULATION

Figure 1: Schematic of a micro channel

Under the action of an external electric field, analyte molecules undergo electrophoretic separation in a microchannel filled with a buffer solution. Consider a channel with width $2b$, depth $2h$, and length L. Without loss of generality, we can assume that $b \geq h$, and hence the aspect ratio $\beta = b/h \geq 1$. We solve the problem using the reference frame shown in Fig. 1, and dimensionless cross-sectional coordinates: $\bar{x} = x/h$, $\bar{y} = y/h$. Let A and Γ denote the normalized cross section and its boundary, respectively.

Under a uniform electric field E along the z-axis, the heat generation density in the buffer is given by $q = E^2 \lambda c$ [6], where λ is the buffer's molar conductivity and c its concentration. Assuming that the channel walls are at room temperature, then heat conduction in the buffer implies that the buffer temperature is above room temperature by

$$\theta = \phi \cdot q h^2 / k \tag{1}$$

where k is the buffer's thermal conductivity. The function ϕ is determined by the following Poisson's equation,

$$\begin{cases} \dfrac{\partial^2 \phi}{\partial \bar{x}^2} + \dfrac{\partial^2 \phi}{\partial \bar{y}^2} = -1 \\ \phi\big|_\Gamma = 0 \end{cases} \tag{2}$$

The buffer temperature is non-uniform within the cross section. Thus, the buffer viscosity, which depends on its temperature, is also non-uniform: $\eta = \eta_w(1 - \alpha\theta)$ [6], where η_w is the viscosity at the channel walls (at room

temperature), and α the buffer's temperature coefficient of viscosity. The electrophoretic mobility of the analyte is inversely proportional to the buffer viscosity [6]: $\mu = \mu_w (\eta_w / \eta) = \mu_w / (1 - \alpha\theta)$, where μ_w is the analyte's electrophoretic mobility at the wall. Assuming that the buffer temperature rise is small, i.e., $\alpha\theta << 1$, it then follows that the analyte velocity is non-uniform within the cross section of the channel,

$$u \approx u_w (1 + \alpha\theta) \tag{3}$$

where u_w is the analyte velocity at the wall.

The analyte concentration $C(\bar{x}, \bar{y}, z)$ in the channel is then determined by the following convective mass transfer equation [8]:

$$\frac{D}{h^2}\left(\frac{\partial^2 C}{\partial \bar{x}^2} + \frac{\partial^2 C}{\partial \bar{y}^2}\right) + D\frac{\partial^2 C}{\partial z^2} = \frac{\partial C}{\partial t} + u \cdot \frac{\partial C}{\partial z} \tag{4}$$

where the left-hand side describes the analyte flux due to diffusion in the presence of a concentration gradient. On the right-hand side of this equation, the first item gives the time rate of concentration change, while the second item represents the analyte flux due to convection [8]. D is the analyte's diffusivity in the buffer and t is time.

3   CLOSED-FORM MODEL

To derive a closed-form model for the convective transport of an analyte due to Joule heating, we make the following classic assumptions of Taylor [3,4]. In these assumptions $\Delta u_{av} = \int_A (u - u_w) \cdot dA / A$ is the relative average velocity of the analyte molecules inside the cross section with respect to those at the channel walls.

I. Longitudinal diffusion is negligible compared with the dispersion caused by JH: $D << h^2 \Delta u_{av}^2 / 48D$. (The right hand side is in fact the same as the dispersion coefficient given in Eq. (9).)

II. The time necessary for appreciable convective transport effects to occur is long compared with the time for transverse concentration variations to effectively reach steady state through molecular diffusion. This assumption can be expressed as $h^2 \Delta u_{av} / 4DL << 1$.

Combining the two assumptions thus requires that $6.9 << \Delta u_{av} / D << 4L/h$ be satisfied. The transverse variation in analyte concentration C can therefore be calculated from Eq. (4) by dropping $\partial^2 C / \partial z^2$ (by assumption I) and $\partial C / \partial t$ (by assumption II)

$$\frac{\partial^2 C}{\partial \bar{x}^2} + \frac{\partial^2 C}{\partial \bar{y}^2} = \frac{(u - u_{av})h^2}{D} \cdot \frac{\partial C}{\partial \xi} \tag{5}$$

where $u_{av} = \int_A u \cdot dA / A$ is the average analyte velocity and $\xi = z - u_{av}t$ is an axial coordinate axis whose origin moves with those analyte molecules that flows with u_{av}. From Eqs. (1)-(3), Eq. (5) can be reformulated to give

$$C = \frac{\alpha q h^4 u_w}{Dk} \cdot \frac{\partial C}{\partial \xi} \Psi \tag{6}$$

where Ψ is determined from

$$\begin{cases} \nabla^2 \Psi = \phi - \phi_{av} \\ \left.\dfrac{\partial \Psi}{\partial n}\right|_\Gamma = 0 \end{cases} \tag{7}$$

When assumption II holds, transverse variations in C are small compared with those in the longitudinal direction. Therefore it is reasonable to assume that $\partial C / \partial \xi$ is approximately the same as $\partial C_{av} / \partial \xi$ [3], where C_{av} is the average concentration over the cross section. Replacing $\partial C / \partial \xi$ with $\partial C_{av} / \partial \xi$ in Eq. (6), the analyte transport flux across the plane $\xi = 0$ is

$$\dot{Q} = -\int_A C(u - u_{av}) \cdot dA = -K\frac{\partial C_{av}}{\partial \xi} \tag{8}$$

where $K = \dfrac{\gamma}{D}\left(\dfrac{\alpha q h^3 u_w}{k}\right)^2$ and $\gamma = \dfrac{1}{4\beta}\int \Psi(\phi - \phi_{av}) \cdot dxdy$.

The continuity equation for the analyte along the longitudinal direction can then be expressed as:

$$K\frac{\partial^2 C_{av}}{\partial \xi^2} = \frac{\partial C_{av}}{\partial t} \tag{9}$$

It can be seen that the dispersion of C_{av} with respect to the $\xi = 0$ (i.e., $x = u_{av}t$) plane is analogous to a molecular diffusion process with a diffusivity K. Therefore, K is the JH dispersion coefficient.

In Eq. (8), all information about cross-sectional geometry is lumped into γ. Hence, after γ is found, the JH dispersion coefficient for different β can be determined.

Fig. 2 shows the dependence of the factor γ on the aspect ratio β. There is an initial increase of γ with β until

γ reaches a maximum. Then γ gradually drops off to a limiting value of 2/945 at $\beta=\infty$, which corresponds to the case of a channel between two parallel plates. Since K is proportional to γ, the JH dispersion follows the same trend as β changes. We will compare these results with numerical simulations in Section 4.

Figure 2: Dependence of γ on the aspect ratio β

4   NUMERICAL SIMULATIONS

All numerical simulations were performed with CoventorWare [9]. We used the software's pressure-flow dispersion module to solve the three-dimensional transport equation (4), with the following analogy that represents Joule heating induced electrophoretic velocity profile in terms of a pressure driven flow velocity profile:

$$\underbrace{\begin{cases} \nabla^2 u = -\dfrac{q}{k}\cdot\alpha u_w \\ u|_\Gamma = u_w \end{cases}}_{Electrophoresis} \Longleftrightarrow \underbrace{\begin{cases} \nabla^2 u = \dfrac{dp}{\eta\cdot dz} \\ u|_\Gamma = u_w \end{cases}}_{Pressure\ Flow} \qquad (10)$$

We consider the three combinations of the electric field strength and channel length as shown in Table 1. The following typical material properties are used [1]: $\mu=5.91\times10^{-8}$ m^{2}V^{-1}s^{-1}, $\eta_w=1.002\times10^{-3}$ m^{2}V^{-1}s^{-1}, $\alpha=0.026$K^{-1}, $k=0.6$ W m^{-1}K^{-1}, $\lambda=0.0332$ m^2 Ω^{-1}mol^{-1}, $c=1$ mM, and $D=3\times10^{-9}$ m^{2}s^{-1}.

No	E (MV/m)	Channel Length (μm)
1	3.16	2040
2	4.22	2040
3	5.28	3040

Table 1: Numerical simulation instances

The analyte's average velocity computed from the parameterized closed-form model introduced in Section 3 matches very well with the numerical simulations results

as shown in Fig. 3. This figure also indicates that JH induces a 2 % nonlinearity in the u_{av} as a function of E.

Figure 3: Average electrophoretic velocity versus E

Tables 2–4 compare the analytically and numerically calculated standard deviation σ at representative times for E=3.16, 4.22 and 5.28 MV/m.

	β=1	β=26/7	β=∞
Num (μm)	11.6	18.7	17.9
Anal (μm)	6.9	16.3	12.96

Table 2: Standard deviation for E=3.16 MV/m (t=9 ms)

	β=1	β=26/7	β=∞
Num (μm)	18.3	33	26.5
Anal (μm)	14.28	33.72	26.84

Table 3: Standard deviation for E=4.22 MV/m (t=6.8 ms)

	β=1	β=26/7	β=∞
Num (μm)	29.6	71.2	53.2
Anal (μm)	30.355	71.64	57.01

Table 4: Standard deviation for E=5.28 MV/m (t=8 ms).

In these tables, for the same electric field E, the standard deviation σ increases initially with β and then decreases. This behavior agrees with the prediction given in Fig. 2. However, large deviations are observed at low E, which can be explained by Fig. 4.

Figure 4: Comparison of K and D versus E

In Fig. 4, K/D provides a comparison of JH convective dispersion and pure axial diffusion. When E=3.16 MV/m, large differences between analytical and numerical results are found. The reason is that at low E, K and D have comparable magnitude, which violates assumption I and renders the analytical model invalid. However, for E=4.22 MV/m and E=5.28 MV/m, the analytical and numerical results agree well. This confirms that for high electric field strengths, JH induced convective dispersion dominates over axial diffusion, and the analytical model is valid.
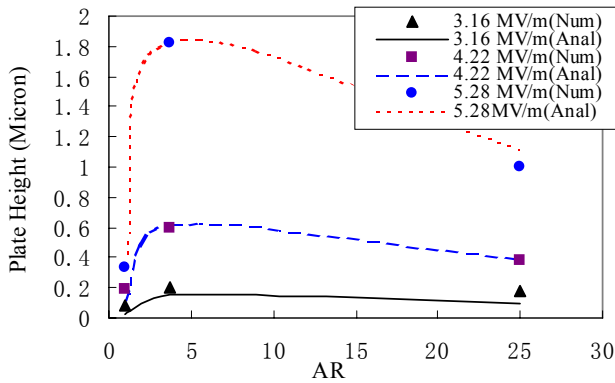
Figure 5: Plate height versus β at different E

The plate height, $H=\sigma^2/L$, where L is the electrophoretic migration distance, is a commonly used time independent measure of separation efficiency [1]. This parameter is used to compare the effect of JH at different field strengths in Fig. 5. We again see a good agreement between the analytical and numerical results (with an error less than 14%). This is true except for E=3.16 MV/m, where assumption I is violated and the analytical model is invalid. In addition, we observe that H increases with E and this phenomenon is more pronounced at large β. For E=5.28 MV/m, H is nearly 2 μm, indicating that JH becomes a significant source of band broadening in microchannels. Finally, Fig. 5 also indicates that existing Joule heating models for a circular tube or a pair of infinitely large parallel plates are inappropriate, since they predict a plate height that is only one-seventh and one-fifth, respectively, of the plate height at β=5.

The reason why band spreading has a maximum around β=5 is not yet clear. According to Eqs. (7) and (8), analyte transport partially depends on θ-θ_{av}, where θ is the difference of the analyte temperature and that of the channel wall, and θ_{av} is θ averaged over the cross section.

Table 5 shows that θ_{max}-θ_{av} also has a maximum with respect to β. It is apparent that the magnitude of the temperature variation θ-θ_{av} across the channel's cross section plays a role in determining JH effects. Work is in progress to clarify this characteristic of band broadening.

β	1	2	4.5	7	∞
θ_{max} (K)	5.57	8.60	9.42	9.44	9.45
θ_{av} (K)	2.66	4.32	5.37	5.73	6.30
θ_{max}-θ_{av} (K)	2.91	4.28	4.05	3.71	3.15

Table 5: θ-θ_{av} across the channel as β varies

5   CONCLUSION

We have presented a parameterized closed form model for dispersion due to Joule heating for use in the design of microchannel electrophoresis systems. The model has been verified using numerical simulation and predicts the effect of cross-sectional shape on Joule heating induced dispersion.

ACKNOWLEDGMENT

REFERENCES

[1] S.C. Jacobson et al. *Anal. Chem.* 70, 3476, 1998.

[2] J.I. Molho et al. *Anal. Chem.* 73, 1350, 2001.

[3] G.I. Taylor. *Proc. Roy. Soc.*, A219, 186, 1953.

[4] G.I. Taylor. *Proc. Roy. Soc.*, A225, 473, 1954.

[5] Aris, R. *Proc. Roy. Soc*, A235, 66, 1956.

[6] J.H. Knox and I.H. Grant. *Chromatographia*, 24: 135-143, 1987.

[7] S.K. Griffiths. *Anal. Chem.* 72, 4767, 2000.

[8] E.L. Cussler. *Diffusion, Mass Transfer in Fluid Systems*, Cambridege Univ. Press, 2nd ed., 1997.

[9] Coventor Inc. *CoventorWare, Microfluidics Tutorials and Reference Guide*, 2001.